ELSEVIER

Polymer 43 (2002) 1835–1847

polymer

www.elsevier.com/locate/polymer

The thermal degradation of PET and analogous polyesters measured by thermal analysis–Fourier transform infrared spectroscopy

B.J. Holland, J.N. Hay*

Plastic Materials Laboratory, School of Metallurgy and Materials, The University of Birmingham, P.O. Box 363, Edgbaston, Birmingham B15 2TT, UK

Received 30 July 2001; accepted 2 November 2001

Abstract

The thermal degradation of two commercial poly(ethylene terephthalate) (PET) samples and two laboratory prepared polyesters, poly(ethylene isophthalate) and poly(diethylene glycol terephthalate), was studied using thermogravimetry and thermal analysis–Fourier transform infrared spectroscopy. The commercial PET samples were copolymerised with diethylene glycol and isophthalic acid groups in different proportions, and their thermal stabilities were found to differ. Through a study of the thermal degradation of poly(diethylene glycol terephthalate) and poly(ethylene isophthalate), it was found that diethylene glycol and isophthalate units promoted thermal degradation through increased chain flexibility and more favourable bond angles, respectively. The thermal degradation of all the polyesters tested lead to the formation of non-volatile residue. Infrared spectroscopic analysis indicated that the residue consisted almost exclusively of interconnected aromatic rings. © 2002 Elsevier Science Ltd. All rights reserved.

Keywords: Poly(ethylene terephthalate); Diethylene glycol; Isophthalic acid

1. Introduction

This publication is concerned with the thermal degradation of poly(ethylene terephthalate) (PET), and the effect of comonomer modifications of PET on thermal stability. Two comonomer modifications were considered: diethylene glycol (DEG) and isophthalic acid (IPA) units. PET is modified in this way to reduce the rate of thermal crystallisation [1,2], which causes the material to appear cloudy, and is undesirable in applications such as soft drink containers.

A number of studies have been made on the thermal degradation of PET [3–11], investigating the major products of degradation of PET reported as carbon dioxide, acetaldehyde, vinyl benzoate, terephthalic acid, terephthaldehydic acid and linear dimers [6–9]. Minor products included carbon monoxide, methane, ethylene, ketene, 1,4-dioxane, toluene, benzaldehyde, divinyl terephthalate and benzoic acid and cyclic oligomers of up to three monomer units in size. The thermal degradation of PET is thought to occur through intramolecular back-biting leading to cyclic oligomers of up to three units in size, and chain scission through a β-C–H hydrogen transfer reaction, leading to vinyl ester and acid end-groups [6–8] (see Fig. 1). Further to this, Villain et al. [10] found evidence that aliphatic end-groups were more susceptible to thermal degradation. PET has also been found to be more susceptible to hydrolysis. In the presence of 0.007% (w:w) water the rate of chain scission at 280 °C was found to be double that of dry material [11].

In this study, the thermal degradation of two samples of commercial PET, one modified by DEG copolymerisation (PET E) and one modified with both DEG and IPA terpolymerisation (PET I) was investigated using thermal analysis–Fourier transform infrared spectroscopy (TA–FTIR) and thermogravimetry (TG). For comparison purposes, poly(diethylene glycol terephthalate) (PDEGT) and poly(ethylene isophthalate) (PEI) were synthesised and subjected to similar degradation experiments.

2. Experimental

Commercial samples of PET were supplied by Eastman Chemical Company and Dupont Chemical Company Ltd, and were assigned PET E and PET I, respectively. PET I was known to contain approximately 2–4 mol% DEG and 1.3–2.6 mol% IPA [12]. Dimethyl sulphoxide was used as a solvent. Methanol, supplied by Aldrich Ltd, was used for extraction of low molecular weight material from PET.

Aldrich Ltd supplied the following as standard laboratory

---

* Corresponding author. Tel.: +44-121-414-4544; fax: +44-121-414-5232.

E-mail address: j.n.hay@bham.ac.uk (J.N. Hay).

PII: S0032-3861(01)00775-3

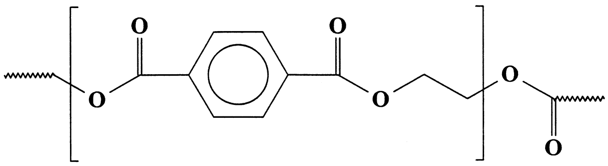

poly(ethylene terephthalate)

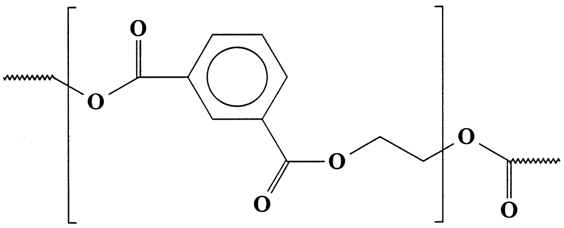

poly(ethylene isophthalate)

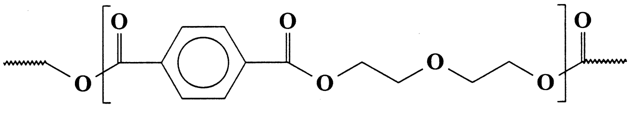

poly(diethylene glycol terephthalate)

Fig. 1. Structural repeat units of PET, PEI and PDEGT.

grade reagents—dimethyl terephthalate, isophthalic acid, ethylene glycol, diethylene glycol, antimony trioxide, calcium acetate, methanol and sulphuric acid for the synthesis of PDEGT and PEI.

TA–FTIR spectroscopy [13] was used to measure the kinetics of polymer degradation, and monitor the changes that occur in the polymer melt during thermal degradation. The apparatus comprised a Linkam 600 hot-stage unit placed in the beam of a Nicolet IR-Magna 760 Fourier Transform infrared spectrometer. The hot-stage unit was fitted with BaF_2 windows suitable for infrared spectroscopy in the region 4000–740 cm^{-1}, and purged for 30 min before each experiment with argon (300 $cm^3\ min^{-1}$). The same flow of argon was maintained throughout the experiment. The temperature of the hot-stage unit was calibrated using the melting point of NaOH and KOH. Degradation of the polyesters was carried out at isothermal temperatures between 200 and 370 °C, using a heating rate from ambient of 90 °C min^{-1}. This allowed the degradation temperature to be achieved before significant degradation had occurred.

Thin films of each polyester were deposited from dilute solution onto KBr disks, and dried in a vacuum oven at 80 °C. Films of the order of 1 μm could be produced in this way. Dimethyl sulphoxide was used as solvent for PET and PEI, whilst chloroform was used as solvent for PDEGT.

For the purposes of kinetic analysis, once the isothermal degradation temperature had been reached, infrared spectra comprising 256 scans were obtained at 10 min intervals. Absorbencies were measured using Nicolet Omnic ESP software.

Isothermal TG was carried out at temperatures between 370 and 410 °C on a Stanton Redcroft 1000 thermogravimetric balance. The hang-down of the balance housed a type R (platinum–rhodium) thermocouple placed close to a platinum sample crucible. A sample size of 30 mg and a 40 $cm^3\ min^{-1}$ flow of argon was chosen. Sample size and gas flow was found to have no effect upon the measured weight loss versus time plots.

3. Copolymer preparations

Dimethyl isophthalate (DMI) was prepared for use in the synthesis of PEI by a method adapted from the literature [14]. Isophthalic acid (10 g) was placed in a flask with 100 cm^3 of methanol and refluxed for 2 h in the presence of 4 cm^3 of concentrated sulphuric acid. On cooling, the reaction mixture was added to 100 cm^3 diethyl ether and 150 cm^3 of water, and shaken. The aqueous layer was discarded. The organic layer was rinsed with 50 cm^3 of water, 50 cm^3 of water with 15% $NaHCO_3$, and with 50 cm^3 of saturated NaCl solution. The organic layer was then dried over Na_2SO_4 for 10 min. DMI was recrystallised from methanol.

Poly(ethylene isophthalate), PEI, was polymerised by a method adapted from the literature [15]. DMI (9.7 g, 0.05 mol), ethylene glycol (EG) (7.1 cm^3, 0.115 mol), Sb_2O_3 (0.04 g) and $Ca(OAc)_2$ (0.015 g) were placed in a 50 cm^3 round bottom flask under nitrogen. The mixture was steadily heated to 170 °C, at which point nitrogen was bubbled through the mixture, being careful that this did not result in volatilisation of the reactants. The reaction mixture should liberate MeOH at this stage, which was removed by distillation. The reaction temperature was then increased to 200 °C for 2 h, and 220 °C to liberate excess EG. The reaction mixture was then placed under vacuum at 280 °C for 3 h to facilitate polymerisation.

During the reaction, Sb_2O_3 is reduced to Sb(0), which gave the polymer a dark appearance when polymerisation was stopped. This was removed by dissolving poly(ethylene isophthalate) in hot DMSO and filtering. The PEI produced was a colourless glass-like solid.

Dimethyl terephthalate (DMT) (9.7 g, 0.05 mol), diethylene glycol (DEG) (12.1 cm^3, 0.115 mol), Sb_2O_3 (0.04 g) and $Ca(OAc)_2$ (0.015 g) were placed in a 50 cm^3 round bottom flask under nitrogen. The mixture was steadily heated to 140 °C, at which point nitrogen was bubbled through the mixture, being careful that this did not result in volatilisation of the reactants. The reaction mixture liberated MeOH at this stage, which was removed by distillation. The reaction temperature was then increased to 200 °C for 2 h, and 220 °C to liberate excess DEG. The reaction mixture was then placed under vacuum at 280 °C for 4 h to facilitate polymerisation. The mixture yellowed during polymerisation, which was probably due to a small amount of degradation, and the reaction was not taken to high conversion. The product was washed with acetone to

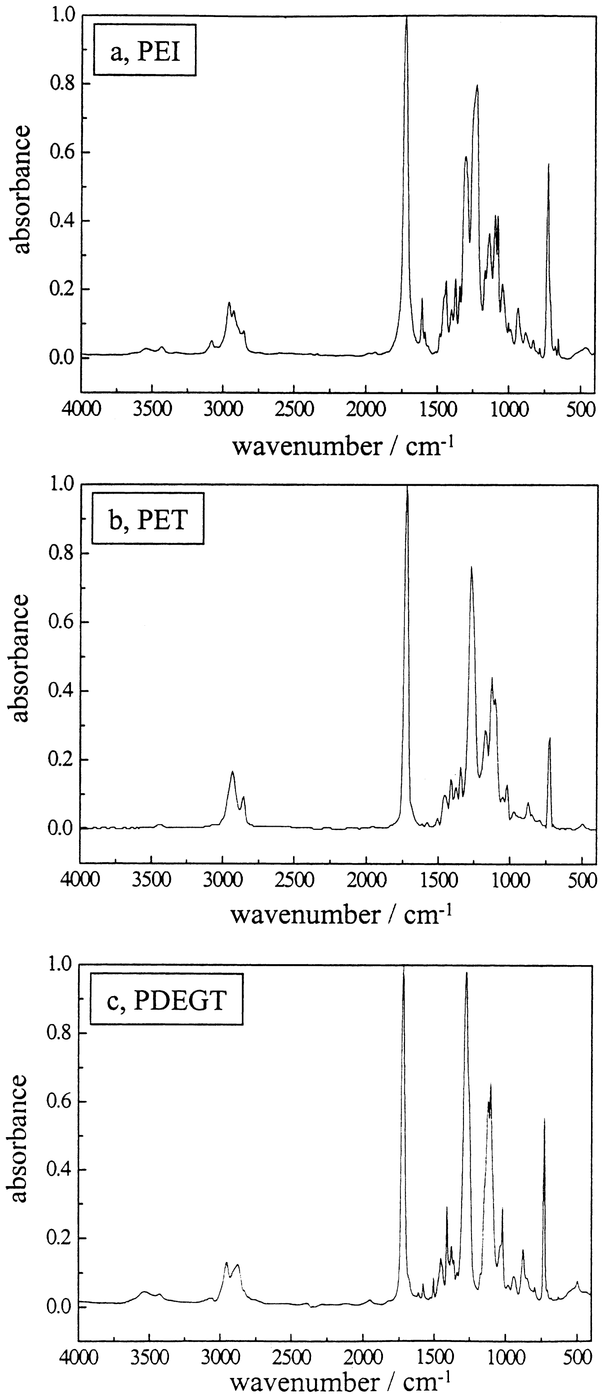

Fig. 2. (a) Infrared spectrum of PEI, (b) infrared spectrum of PET, and (c) infrared spectrum of PDEGT.

remove impurities. The resulting polymer was a soft, sticky, slightly yellow material, which became solid and brittle after several months.

4. Confirmation of structure of the polyesters

Table 1
Band assignations for the infrared spectrum of poly(ethylene isophthalate)

Wavenumber (cm^{-1})	Assignment
3440	O–H stretching of ethylene glycol end-group
3060	Aromatic C–H stretching
2960, 2860	Aliphatic C–H stretching
1730	Carbonyl C=O stretching
1600, 1450, 1430	Aromatic skeletal stretching bands [16]
1465	$-CH_2-$ deformation
1295	Unknown
1220	C(O)–O stretching in ester
1165, 1090, 1070	Bands in this region are indicative of aromatic substitution pattern, and 1,3-substitution [17]
930	C–H deformation of a lone uncoupled hydrogens on an aromatic ring [18]
820	C–H deformation of three adjacent coupled hydrogens on an aromatic ring [18]
730	Probably associated with the out of plane deformation of two aliphatic substituents of the aromatic ring

The structural repeat unit of poly(ethylene isophthalate) is shown in Fig. 1. The polymer produced was clear and colourless once all of the antimony catalyst had been removed from the sample. Its structure was confirmed by infrared spectroscopy (see Fig. 2a and Table 1). For comparison, an infrared spectrum of poly(ethylene terephthalate) (PET) is shown in Fig. 2b, and assignments shown in Table 2.

The structural repeat unit of poly(diethylene glycol terephthalate) is shown in Fig. 1. The polymer became slightly yellow during the early stages of transesterification, an indication of the early stages of degradation. For this

Table 2
Band assignments for the infrared spectrum of poly(ethylene terephthalate)

Wavenumber (cm^{-1})	Assignment
3535	Absorbed moisture
3440	O–H stretching of diethylene glycol end-group
3060	Aromatic C–H stretching
2960, 2880	Aliphatic C–H stretching
1950	Aromatic summation band
1720	Carbonyl C=O stretching
1615, 1450, 1430, 1410	Aromatic skeletal stretching bands [16]
1950	Aromatic summation band
1720	Carbonyl C=O stretching
1615, 1450, 1430, 1430	Aromatic skeletal stretching bands [16]
1465	$-CH_2-$ deformation band
1270	C(O)–O stretching of ester group
1175, 1120 and 1020	Bands in the skeletal ring region are indicative of aromatic substitution pattern, and indicates 1,4-substitution [17]
980	$O-CH_2$ stretching of ethylene glycol segment in PET
850	C–H deformation of two adjacent coupled hydrogens on an aromatic ring [18]
730	Associated with the out of plane deformation of the two carbonyl substituents on the aromatic ring [18]

Table 3
Band assignments for the infrared spectrum of poly(diethylene glycol terephthalate)

Wavenumber (cm^{-1})	Assignment
3535	Absorbed moisture
3440	O–H stretching of diethylene glycol end-group
3060	Aromatic C–H stretching
2960, 2880	Aliphatic C–H stretching. 2880 cm^{-1} band intense compared to that in PET, and is probably associated with an additional aliphatic C–H environment in the diethylene glycol segment
1950	Aromatic summation band
1720	Carbonyl C=O stretching
1615, 1450, 1430, 1410	Aromatic skeletal stretching bands [16]
1580	May be associated with skeletal ring breathing, or onset of small amount of degradation during polymerisation
1465	$-CH_2-$ deformation band
1270	C(O)–O stretching of ester group
1175, 1120 and 1020	Bands in the skeletal ring region are indicative of aromatic substitution pattern, and indicates 1,4-substitution [17]
980	$O-CH_2$ stretching of ethylene glycol segment in PET
940	Not present in PET. May be associated with $O-CH_2$ stretching [17] of DEG segment
870	C–H deformation of two adjacent coupled hydrogens on an aromatic ring [18]
730	Associated with the out of plane deformation of the two carbonyl substituents on the aromatic ring [18]

reason, the reaction was not taken to high molecular weight. The polymer produced was slightly yellow, clear and tacky at room temperature, although after a period of several months the material solidified and became opaque, indicative of crystallisation. An infrared spectrum of PDEGT is shown in Fig. 2c, and assignments are given in Table 3.

5. Study of the thermal degradation of polyesters by TA–FTIR spectroscopy

TA–FTIR spectroscopy was carried out on samples of PET deposited on KBr disks, as described in Section 3. Isothermal degradation temperatures between 350 and 370 °C were used, and the spectra were measured at 10 min intervals. Typical degradation experiments using PET I at 370 °C are shown in Fig. 3, and the same experiment with PET E gave similar results. The change in intensity of selected infrared bands is shown in Fig. 4. A new infrared band evolved at 1560 cm^{-1}, the appearance of which coincided with changes in the $C-H_{(def)}$ region (950–750 cm^{-1}) of the infrared spectrum. The band at 1560 cm^{-1} is related to build-up of a conjugated aromatic structure in the polymer residue. The changes in the $C-H_{(def)}$ region were symptomatic of changes in the substitution pattern of the aromatic ring in PET. The band at 870 cm^{-1}, associated with the $C-H_{(def)}$ of two adjacent hydrogens (indicating 1,4 substitution) diminished, whilst simultaneously a band at 823 cm^{-1} evolved. This band was probably due to the $C-H_{(def)}$ of three adjacent hydrogens on the aromatic ring. A second, less intense band also built-up at 880 cm^{-1} during thermal degradation, which is within the range associated with the $C-H_{(def)}$ of one lone hydrogen. In addition a third new band was observed at 742 cm^{-1}, which was probably due to the $C-H_{(def)}$ mode

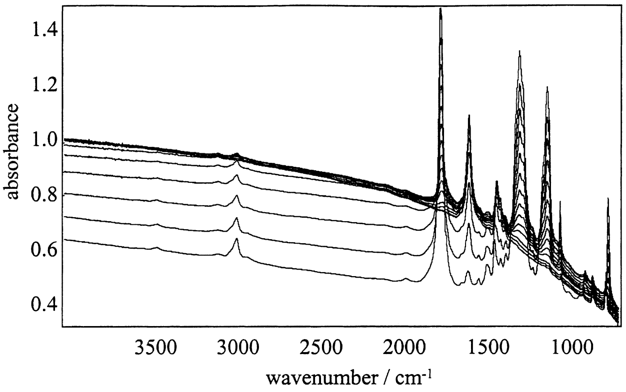

Fig. 3. Evolution of infrared spectra of PET E at 370 °C.

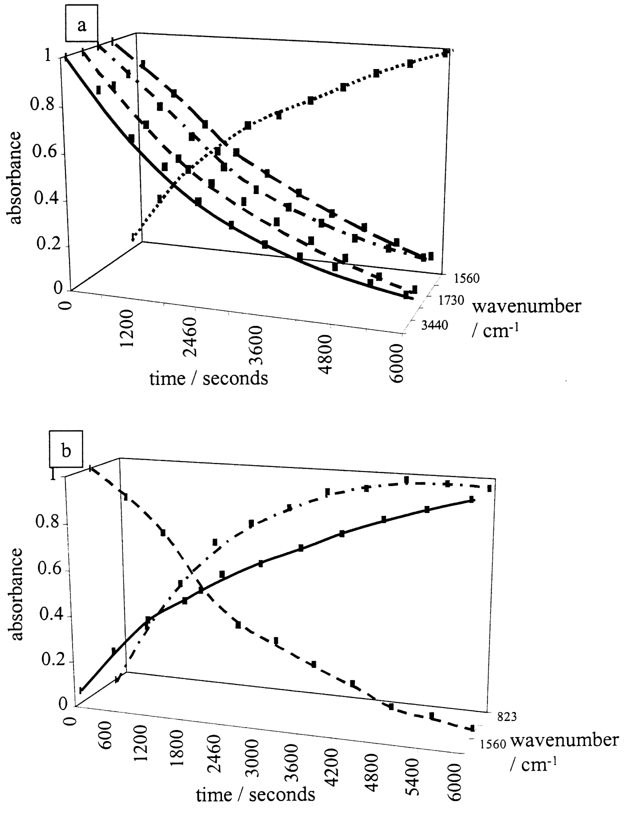

Fig. 4. Change in intensity of selected infrared bands of PET E at 370 °C, (a) 3440–1560 cm^{-1}: (—) 3440 cm^{-1}, (- - -) 2960 cm^{-1}, (-·-·-) 1730 cm^{-1}, (– – –) 1250 cm^{-1}, (···) 1560 cm^{-1}. (b) 1560–823 cm^{-1}: (—) 1560 cm^{-1}, (- - -) 868 cm^{-1}, (-·-·-·-) 823 cm^{-1}.

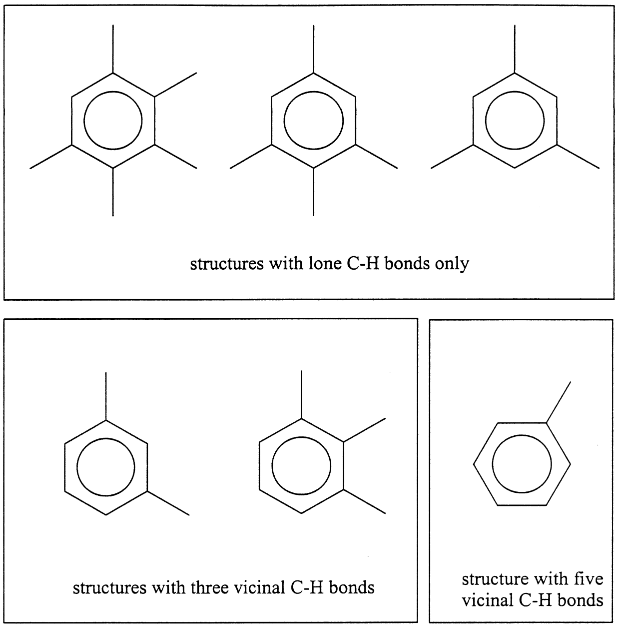

Fig. 5. Possible aromatic ring structures in the non-volatile residue of PET.

of five adjacent C–H groups, and was the most intense of the three bands.

The changes observed in the C–H$_{(def)}$ region at 880 and 823 cm^{-1} may indicate that the structure of the aromatic ring changed from 1,4 to 1,3. However, in PEI, the intensity of the band at 880 cm^{-1} was approximately the same intensity as the band at 823 cm^{-1}, but in the infrared spectrum of the final non-volatile residue, the band at 823 cm^{-1} was approximately four times more intense than the band at 880 cm^{-1}. This was an indication that there were only a small number of aromatic rings with one uncoupled C–H, compared to the number of aromatic rings with three adjacent C–H groups. This could mean that most of the aromatic rings in the non-volatile residue were 1,2,3 vicinal trisubstituted. This was consistent with the conjugated aromatic band occurring at relatively low wavenumber (1560 cm^{-1}) [19], rather than being close to 1600 cm^{-1}. In addition, the band at 740 cm^{-1} was probably due to the C–H$_{(def)}$ of five vicinal hydrogens, and was therefore evidence that the final structure was terminated with phenyl rings. Although the actual structure of the non-volatile residue could not be deduced fully from the results shown here, the possible substitution patterns of the aromatic rings are shown in Fig. 5.

Elsewhere in the infrared spectrum, there was evidence that PET degraded to a product that probably consisted mostly of aromatic rings. Whilst the aliphatic C–H$_{(str)}$ band (2960 cm^{-1}), the carbonyl band (1730 cm^{-1}) and the ester band (1255 cm^{-1}) diminished with time, the ring breathing modes of the aromatic ring in the region 1410–1330 cm^{-1} were retained, although there were shifts in their wavenumbers, probably due to changes in the substitution patterns of the aromatic rings.

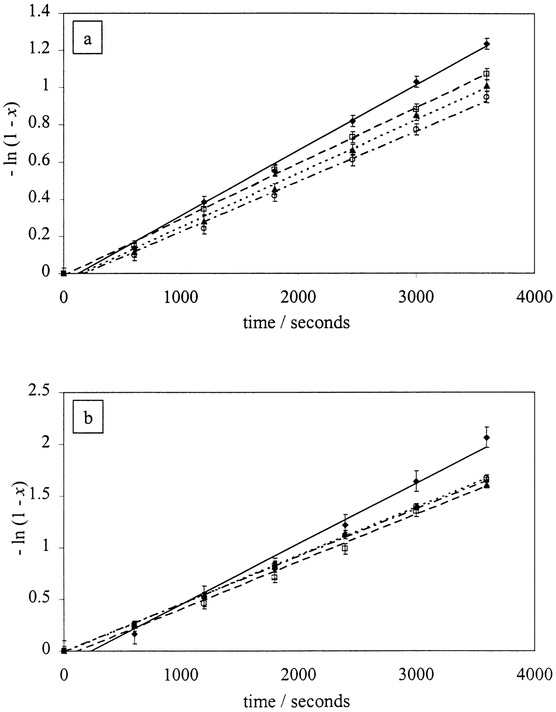

Fig. 6. First order rate plots of the loss in intensity of selected infrared bands of (a) PET E and, (b) PET I. (—◆—) 3440 cm^{-1}, (--□--) 2960 cm^{-1}, (---▲---) 1730 cm^{-1}, (---○---) 1250 cm^{-1}.

The kinetics of the thermal degradation at 350–370 °C were measured by TA–FTIR spectroscopy. First order rate plots of the rate of disappearance of bands at 3440 (probably end-group O–H$_{(str)}$), 2960 (aliphatic C–H$_{(str)}$), 1730 (C=O$_{(str)}$) and 1225 (ester) cm^{-1} at 370 °C are shown in Fig. 6, for PET E and PET I, respectively. It was found that certain other infrared bands did not follow first order kinetics. These included the loss of the C–H$_{(def)}$ band for two vicinal hydrogens (870 cm^{-1}), the build-up of the C–H$_{(def)}$ band for three vicinal hydrogens (823 cm^{-1}), and the build-up of conjugated aromatic structure (1560 cm^{-1}). These bands appeared to follow half order kinetics (see Fig. 7 for PET E and PET I at 370 °C). The rate of loss of the band at 870 cm^{-1} was greater than the rate of gain of 823 cm^{-1}. This was probably due to aromatic material volatilising by a first order weight loss process, and also produced the slight curvature observed in the rate plot for loss of the band at 870 cm^{-1}.

The thermal degradation of PET which leads to the production of volatile material has been rationalised into two degradation processes, intramolecular back-biting, and β-C–H hydrogen transfer, as shown in Fig. 8. The intramolecular back-biting process leads to cyclic oligomers, and would cause a proportionate loss in all infrared bands, but the β-C–H hydrogen transfer process does not cause a proportionate loss. Kinetic data for PET E and PET I (see Tables 4 and 5), showed that the three bands, 2960, 1730 and 1225 cm^{-1}, all representing a different part of the molecule, were lost at the same rate. This was considered to

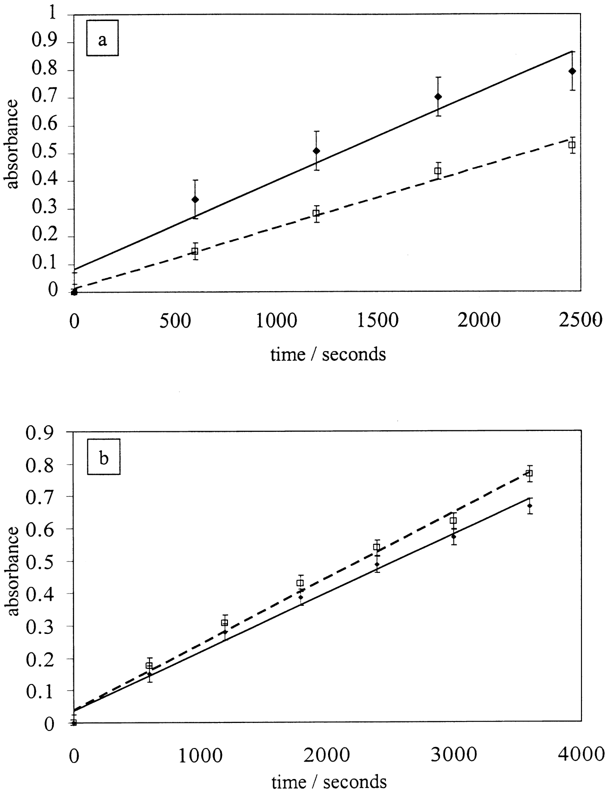

Fig. 7. Half order rate plots of the change in intensity of selected infrared bands of (a) PET E and, (b) PET I. (—◆—) 868 cm^{-1}, (--◻--) 823 cm^{-1}.

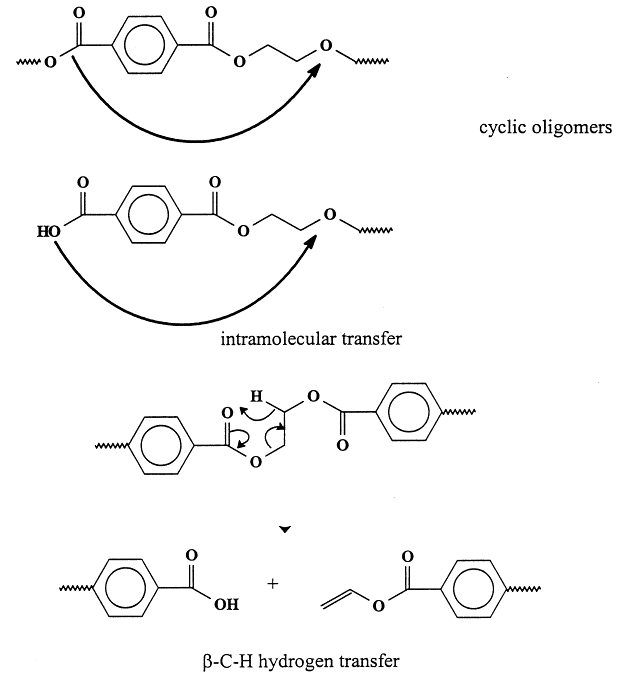

Fig. 8. Mechanisms of thermal degradation of PET reported in the literature.

Table 4
Kinetic data for the thermal degradation of PET E by TA–FTIR spectroscopy

Temperature (°C)	Rate constant for loss of C–H (s^{-1})	Rate constant for loss of C=O (s^{-1})	Rate constant for loss of ester (s^{-1})	Rate constant for loss of ethylene glycol end-group (s^{-1})
350	1.52	1.61	1.71	2.42
355	2.19	2.11	2.06	2.98
360	2.87	3.11	2.92	4.01
365	4.46	4.41	4.22	5.06
370	6.04	6.17	6.19	6.27
Activation energy (kJ mol^{-1})	230 ± 10	220 ± 10	220 ± 10	160 ± 10
Pre-exponential factor (s^{-1})	$(3.62 \pm 0.35) \times 10^{15}$	$(2.05 \pm 0.21) \times 10^{15}$	$(3.58 \pm 0.39) \times 10^{14}$	$(9.37 \pm 1.0) \times 10^{9}$

Table 5
Kinetic data for the thermal degradation of PET I by TA–FTIR spectroscopy

Temperature (°C)	Rate constant for loss of C–H (s^{-1})	Rate constant for loss of C=O (s^{-1})	Rate constant for loss of ester (s^{-1})	Rate constant for loss of ethylene glycol end-group (s^{-1})
350	1.00	0.83	0.88	2.30
355	1.32	1.38	1.40	3.05
360	1.77	1.83	1.78	3.92
365	2.57	2.61	2.67	4.67
370	4.48	4.38	4.38	6.06
Activation energy (kJ mol^{-1})	240 ± 10	260 ± 10	260 ± 10	160 ± 10
Pre-exponential factor (s^{-1})	$(2.56 \pm 0.27) \times 10^{16}$	$(1.16 \pm 0.14) \times 10^{18}$	$(2.92 \pm 0.30) \times 10^{17}$	$(3.77 \pm 0.40) \times 10^{9}$

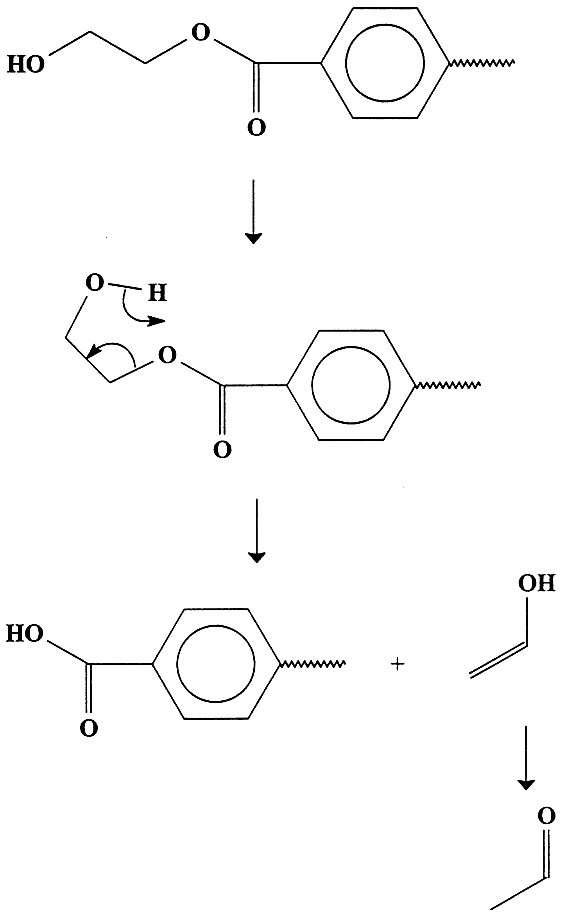

Fig. 9. Degradation of an ethylene glycol end-group to form acetaldehyde and an acid end-group.

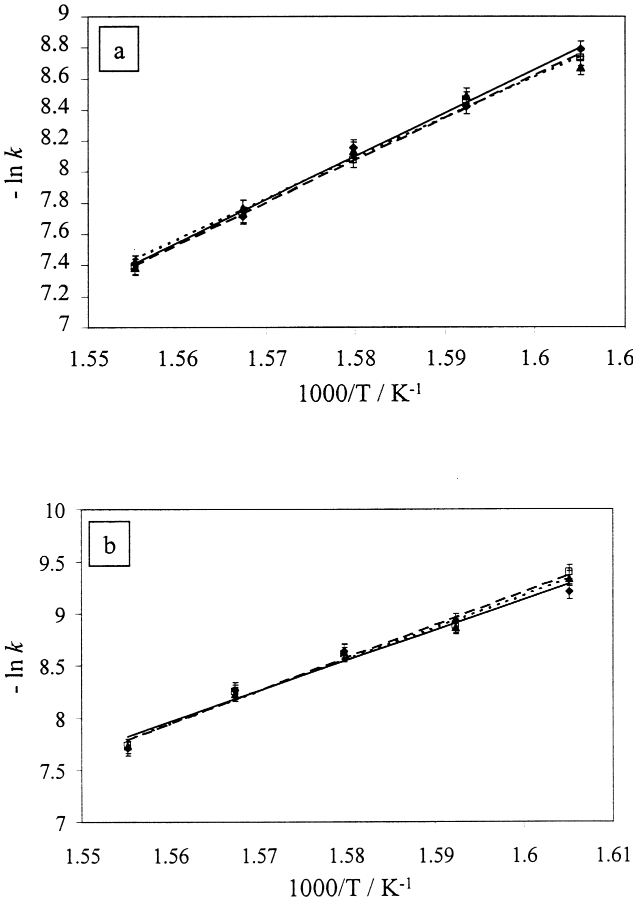

Fig. 10. Arrhenius plot for the thermal degradation of (a) PET E and (b) PET I. (—◆—) 2960 cm^{-1}, (--⊟--) 1730 cm^{-1}, (---▲---) 1250 cm^{-1}.

be an indication that the intramolecular back-biting process was favoured at the temperatures used. Alternatively, this could mean that the β-C–H hydrogen transfer process subsequently led to loss of monomer units. It was considered likely that the loss in the three infrared bands mentioned was due to a combination of both processes, hence the kinetic parameters calculated reflected both processes. It should also be noted that it was difficult to ascertain whether a proportionate amount of aromatic segments were lost due to the shifts in band position around 1400 cm^{-1} during thermal degradation. Given that it has been proposed earlier in this chapter that aromatic segments from PET make up part of the aromatic structure, it is probable that as the reaction proceeds, more aliphatic parts of PET are lost than aromatic parts, and this will also be reflected in the kinetic data.

A fourth band at 3440 cm^{-1}, thought to be related to the ethylene glycol derived end-groups of the polymer, was found to degrade at a different rate to the other three bands. Its disappearance probably led to the formation of acetaldehyde (see Fig. 9).

Arrhenius plots were constructed in order to calculate the activation energy and pre-exponential factor for the loss of the bands at 2960, 1730 and 1255 cm^{-1} for PET E and PET I (Fig. 10). The average activation energy was 230 ± 10 and 250 ± 10 kJ mol^{-1}, for PET E and PET I, respectively. These values were considered to be similar to one another within experimental error. The pre-exponential factor was $(1.4 \pm 0.1) \times 10^{15}$ and $(2.1 \pm 0.2) \times 10^{17}$ s^{-1}, for PET E and PET I, respectively. The pre-exponential factor was higher for PET I, and as a result the rate constants for thermal degradation of PET I were higher than for PET E.

The Arrhenius plots for the loss of the band at 3440 cm^{-1} are shown in Fig. 11. The activation energy was found to be 160 ± 10 kJ mol^{-1} for PET E and PET I. The pre-exponential factor was $(9.37 \pm 1.0) \times 10^{9}$ and $(3.77 \pm 0.4) \times 10^{9}$ s^{-1}, for PET E and PET I, respectively. It was considered that this band was associated with ethylene glycol end-groups, and the results illustrate the lability of ethylene glycol end-groups to thermal degradation. Loss of such an end-group would lead to the formation of a carboxylic acid end-group, the reactivity of which may promote intramolecular back-biting.

The loss of the infrared band at 870 cm^{-1} ($C–H_{(def)}$ two vicinal hydrogens), and the build-up of infrared band at 823 cm^{-1} ($C–H_{(def)}$ of three vicinal hydrogens), were

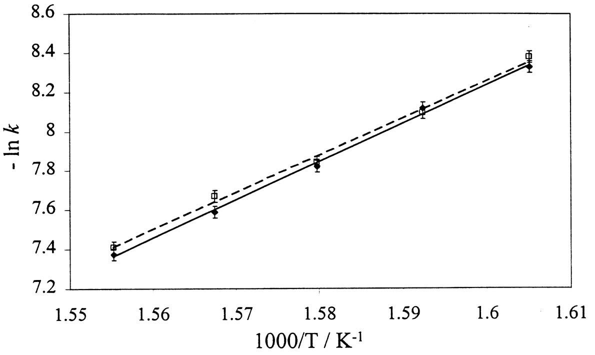

Fig. 11. Arrhenius plot for the thermal degradation of ethylene glycol end-groups of PET E and PET I. (—◆—) PET E, (--□--) PET I.

found to follow half order kinetics. The reason why half order kinetics were observed may have been due to the electron withdrawing effect of the substituents of the benzene ring of PET, which increases the pK_a of the hydrogens *ortho* to them. Hence, if the reaction considered here required an *ortho* hydrogen from the benzene ring to dissociate to produce a reactive species, the following equilibrium must be observed,

$$\Phi - \mathrm{H} \rightleftharpoons \Phi^- + \mathrm{H}^+$$

$$K = \frac{[\Phi - \mathrm{H}]}{[\Phi^-][\mathrm{H}^+]}$$

where K is the equilibrium constant, $[\Phi - \mathrm{H}]$ is the concentration of undissociated *ortho* hydrogen, $[\mathrm{H}^+]$ is the concentration of dissociated protons and $[\Phi^-]$ is the concentration of reactive benzene species in PET. As $[\mathrm{H}^+] = [\Phi^-]$,

$$[\Phi^-]^2 = \frac{[\Phi - \mathrm{H}]}{K}$$

and hence,

$$[\Phi^-] = \left(\frac{[\Phi - \mathrm{H}]}{K}\right)^{1/2}$$

Therefore, if the reaction which lead to non-volatile residue formation in PET required the reactive species, Φ^-, the concentration of Φ^- would have a half order dependence on the total concentration of benzene in PET. Alternatively, a radical degradation process with a bimolecular termination step would also lead to half order kinetics, i.e.

$$2\mathrm{R}^{\cdot} \rightleftharpoons \mathrm{R–R}$$

Possible mechanisms by which PET is converted to non-volatile residue will be discussed in Section 7.

The kinetic parameters for the thermal degradation of PET associated with half order kinetics are shown in Tables 6 and 7, for PET E and PET I, respectively. The related Arrhenius plots are shown in Fig. 12. In the case of PET E, the activation energy for the loss of the band at 870 cm^{-1}, and build-up at 823 cm^{-1} was 190 ± 10 and 220 ± 10 kJ mol^{-1}, respectively. In the case of PET I, the activation energy for the loss of the band at 870 cm^{-1}, and build-up at 823 cm^{-1} was 200 ± 10 and 215 ± 10 kJ mol^{-1}, respectively. The difference in rate constant for each process can be seen in Tables 6 and 7, where the rate of loss of the band at 870 cm^{-1} was approximately double that for the build-up at 823 cm^{-1}. The difference between the loss of

Table 6
Half order kinetic data for the thermal degradation of PET E

Temperature (°C)	Rate constant for loss of 870 cm^{-1} band (× 10^{4} s^{-1})	Rate constant for build-up of 823 cm^{-1} band (× 10^{4} $^{-1}$)
350	0.98	0.45
355	1.19	0.70
360	1.71	1.01
365	1.96	1.26
370	3.27	1.72
Activation energy (kJ mol^{-1})	190 ± 10	220 ± 10
Pre-exponential factor (s^{-1})	(1.69 ± 0.20) × 10^{12}	(9.22 ± 0.95) × 10^{13}

Table 7
Half order kinetic data for the thermal degradation of PET I

Temperature (°C)	Rate constant for loss of 870 cm^{-1} band (× 10^{4} s^{-1})	Rate constant for build-up of 823 cm^{-1} band (× 10^{4} $^{-1}$)
350	1.00	0.48
355	1.28	0.70
360	1.78	0.95
365	2.06	1.30
370	3.54	1.75
Activation energy (kJ mol^{-1})	200 ± 10	215 ± 10
Pre-exponential factor (s^{-1})	(5.33 ± 0.60) × 10^{12}	(4.44 ± 0.48) × 10^{13}

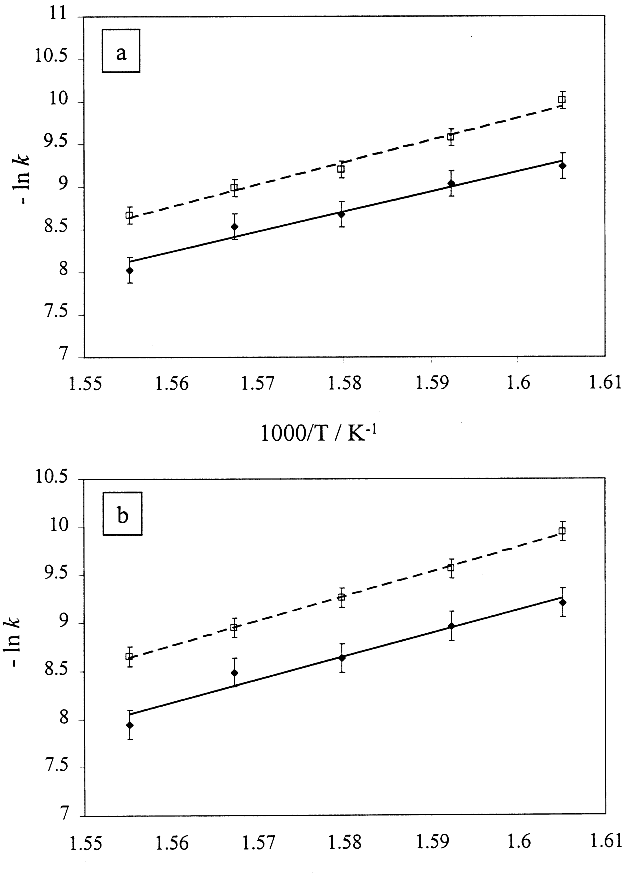

Fig. 12. Arrhenius plots for half order changes in (a) PET E and (b) PET I. (—◆—) 868 cm^{-1}, (--□--) 823 cm^{-1}.

the band at 868 cm^{-1} and the build-up at 823 cm^{-1} was thought to be due to the contribution of volatile degradation processes to the loss of the 870 cm^{-1} band.

The degradation of poly(ethylene isophthalate) (PEI) was studied isothermally by TA–FTIR, as described in Section 3, at temperatures between 320 and 350 °C. The evolution of the infrared spectra with time at 340 °C is shown in Fig. 13, and the change in intensity of selected bands shown in Fig. 14a. First order rate plots for the loss of intensity of infrared bands at 3440, 2960, 1730 and 1220 cm^{-1} are shown in Fig. 14b. They were all linear within experimental error. With increasing extent of thermal degradation of PEI, a new infrared band at 1560 cm^{-1}, assigned to aromatic or conjugated products, built-up progressively, but the intensity was a fraction of that observed during the thermal degradation of PET. Furthermore, the band at 1600 cm^{-1}, which was probably related to the concentration of aromatic rings in the polymer, did not disappear as quickly as most other bands, indicating that a non-volatile residue was formed from the benzene rings of PEI. No new bands were observed in the C–H$_{(def)}$ region of the infrared spectrum.

The first order rate constants for loss of the bands at 2960, 1730 and 1220 cm^{-1} were averaged, and used to calculate the activation energy for the loss of volatile products during the thermal degradation of PEI from the Arrhenius plot (Fig. 15). The activation energy was found to be 200 ± 10 kJ mol^{-1}, and the pre-exponential factor was

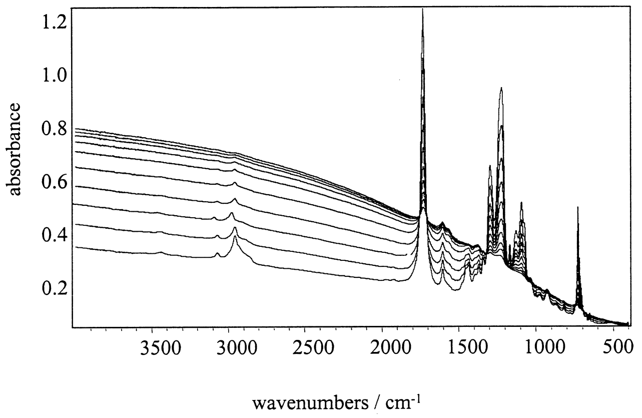

Fig. 13. Evolution of infrared spectra of PEI at 340 °C.

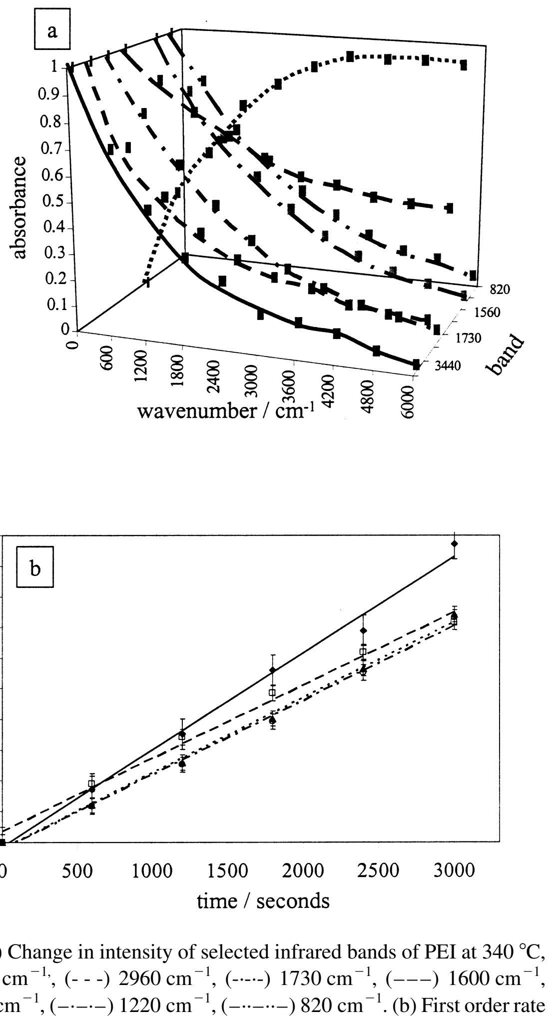

Fig. 14. (a) Change in intensity of selected infrared bands of PEI at 340 °C, (—) 3440 cm^{-1}, (- - -) 2960 cm^{-1}, (-·-·-) 1730 cm^{-1}, (– – –) 1600 cm^{-1}, (···) 1560 cm^{-1}, (–·–·–) 1220 cm^{-1}, (–··–··–) 820 cm^{-1}. (b) First order rate plot for loss in intensity of selected infrared bands of PEI at 340 °C. (—◆—) 3440 cm^{-1}, (--□--) 2960 cm^{-1}, (---▲---) 1730 cm^{-1}, (---○---) 1250 cm^{-1}.

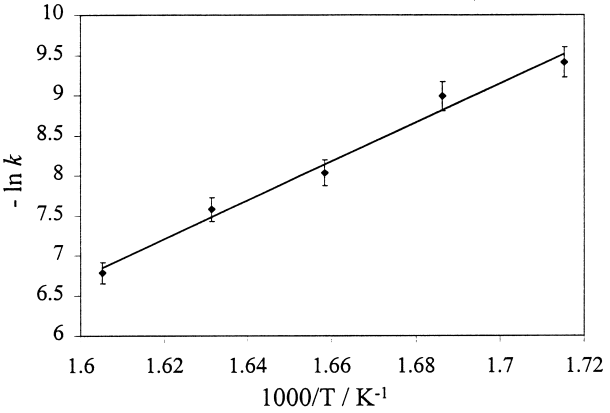

Fig. 15. Arrhenius plot for the thermal degradation of PEI.

$(7.9 \pm 0.5) \times 10^{13}\ s^{-1}$. The values for activation energy and pre-exponential factor calculated for PEI were lower than those found for PET E and PET I, due to the *meta* structure of the aromatic ring, which would have allowed the chain to back-bite more readily than with the *para* structure of PET.

Poly(diethylene glycol terephthalate) (PDEGT) was degraded between 200 and 300 °C. The evolution of the infrared spectra with time at 200 °C is shown in Fig. 16. The infrared spectrum of PDEGT was similar to that of PET, with the notable exception of bands at 2880 and 980 cm^{-1}, see Section 4. An experimental difficulty arose, which was believed to be caused by the low viscosity of the PDEGT, which allowed it to flow during the thermal degradation. Understandably, this caused difficulty in measuring kinetics of thermal degradation by TA–FTIR spectroscopy. The effect was minimised by using very thin samples, but it did not completely prevent it. For this reason, the kinetics of thermal degradation of PDEGT will not be reported.

As can be seen in Fig. 16, at 200 °C PDEGT degraded at lower temperatures than either PET or PEI. It lead to an proportional loss in all infrared bands, although it was found that a new band evolved at 3315 cm^{-1}, reaching a maximum intensity at 30 min, before reducing in intensity. This was assigned to the presence of carboxylic acid end-group $O{-}H_{(str)}$. A weak band at 1560 cm^{-1} also evolved, and was assigned to the build-up of small amounts of conjugated aromatic material, similar to that observed in PET.

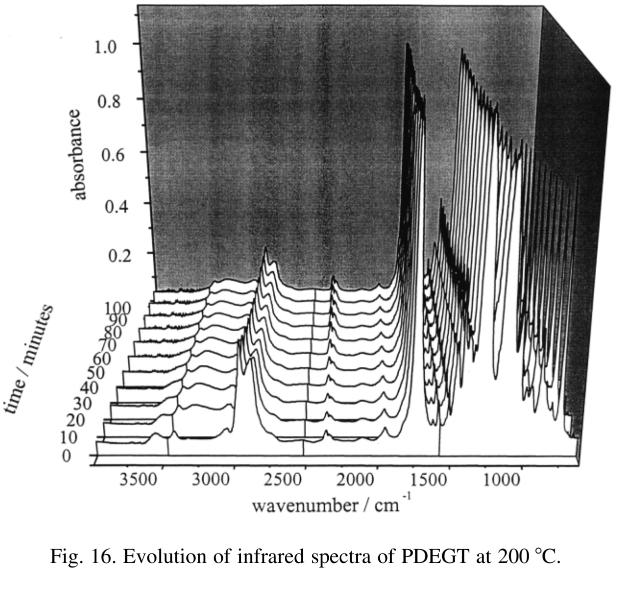

Fig. 16. Evolution of infrared spectra of PDEGT at 200 °C.

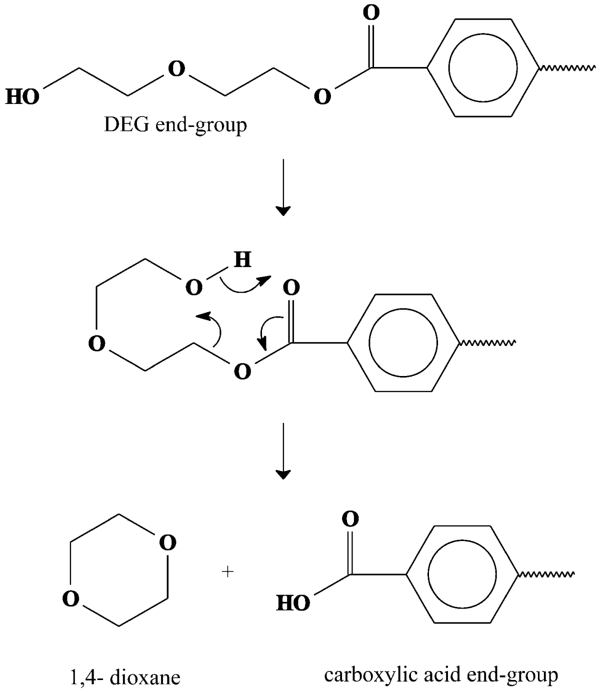

Fig. 17. Degradation of a diethylene glycol end-group giving 1,4-dioxane and a carboxylic acid end-group.

In this study, it was found that a band assigned to ethylene glycol end-group $O{-}H_{(str)}$, decayed more quickly than other infrared bands in the spectrum PET during degradation. It was considered that these groups degraded, by releasing acetaldehyde, and leaving acid end-groups. It was thought that the same type of reaction occurred during the degradation of PDEGT, leading to 1,4-dioxane and an acid end-group (see Fig. 17). The acid end-groups would then decarboxylate, releasing CO_2, or back-bite along the polymer chain. Carboxylic acid end-groups were only observed during the degradation of PDEGT since it was a much lower molecular weight than PET E and PET I, and therefore contained more end-groups.

The evolution of the infrared spectra during the thermal degradation of PDEGT at 300 °C is shown in Fig. 18. It was found that a small quantity of carboxylic acid end-groups developed instantaneously, but began to decrease almost immediately. Thermal degradation at 300 °C lead to the production of a more intense band at 1560 cm^{-1}, indicating that more non-volatile residue was produced. Furthermore, changes in the $C{-}H_{(def)}$ region of the indicated that non-volatile residue was formed from PDEGT in the same way as that of PET.

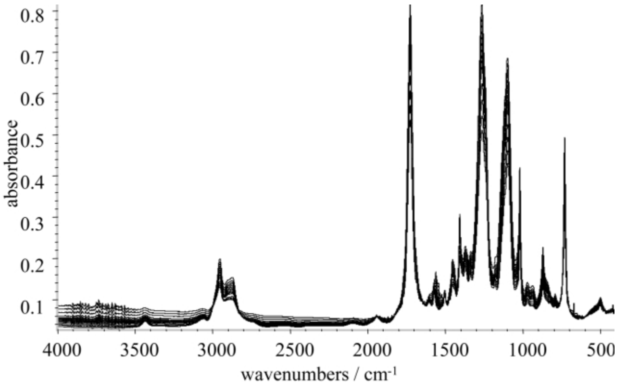

Fig. 18. Evolution of infrared spectra of PDEGT at 300 °C.

6. Thermogravimetric analysis of polyesters

Samples of PET E, PET I, PEI and PDEGT were degraded isothermally by TG in the temperature range 370–410 °C. In each case, a first order dependence on residual weight was observed, and the constants were calculated from the initial linear portion, see Fig. 19. A list of first order rate constants is given in Table 8. Arrhenius plots from the rate constants for the four polyesters are shown in Fig. 20, and the activation energies for the weight loss of PET E, PET I, PEI and PDEGT, were found to be 200 ± 10, 220 ± 10, 190 ± 10 and 190 ± 10 kJ mol^{-1}, respectively. The pre-exponential factors for PET E, PET I, PEI and PDEGT were $(1.17 \pm 0.15) \times 10^{12}$, $(3.17 \pm 0.31) \times 10^{13}$, $(6.53 \pm 0.65) \times 10^{11}$ and $(5.46 \pm 0.68) \times 10^{11}$ s^{-1}, respectively.

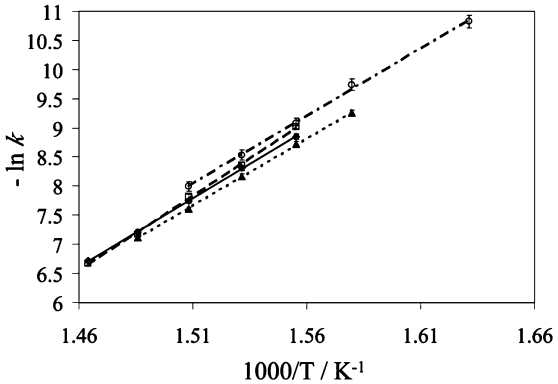

Fig. 20. Arrhenius plot for the thermal degradation of polyesters by TG. (—◆—) 3440 cm^{-1}, (--□--) 2960 cm^{-1}, (—▲—) 1730 cm^{-1}, (---○---) 1250 cm^{-1}.

Similar activation energies were calculated for PEI and PDEGT, and it was considered that their stabilities, in terms of weight loss, were similar. PET E and PET I were more stable than PEI or PDEGT, and it was considered that diethylene glycol and isophthalate segments facilitated a back-biting thermal degradation process, through increased chain flexibility and more favourable bond angles, respectively. There was a clear difference between the kinetic parameters of PET E and PET I. The lower activation energy of thermal degradation of PET E may have been due to diethylene glycol segments having a greater effect in reducing the thermal stability than the isophthalate units, although the thermal stability of PEI and PDEGT has been found to be similar. Therefore, it was considered more likely

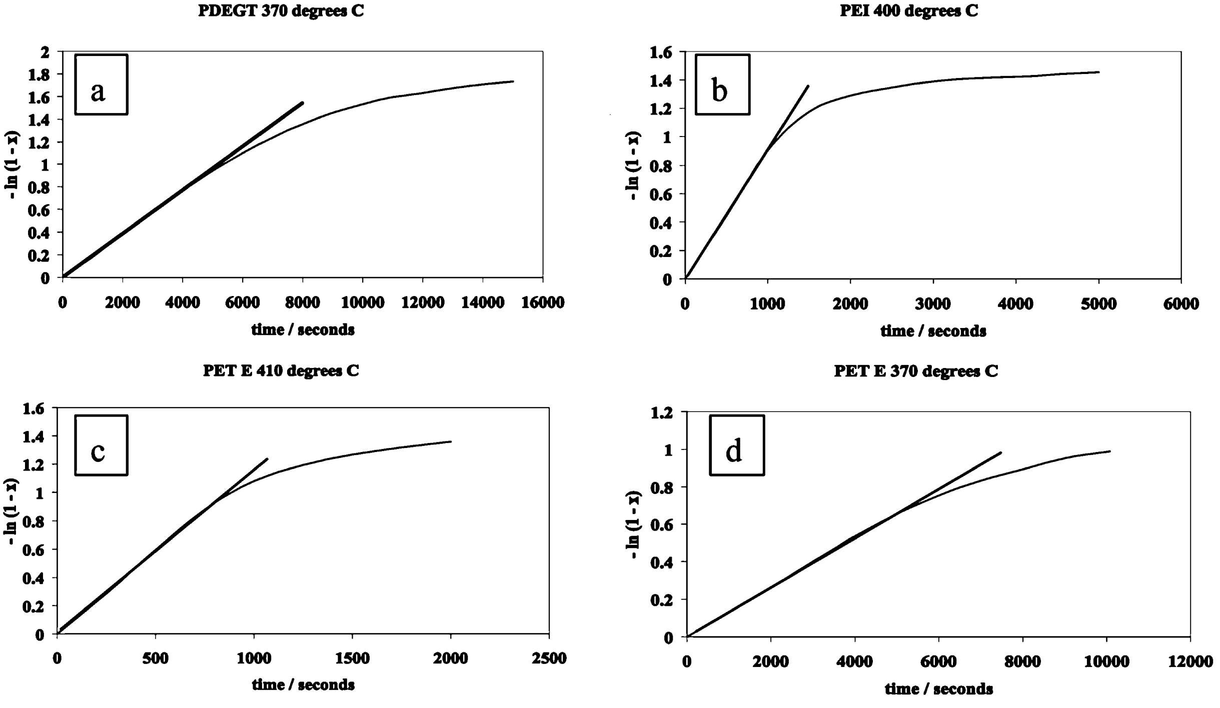
PDEGT 370 degrees C

PEI 400 degrees C

PET E 410 degrees C

PET E 370 degrees C

Fig. 19. First order rate plots for polyesters from TG data.

Table 8
Kinetic data for the thermal degradation of polyesters, measured by TG

Temperature (°C)	First order rate constants for weight loss ($\times 10^4$ s^{-1})			
	PET E	PET I	PEI	PDEGT
340				0.20
360			0.95	0.59
370	1.44	1.21	1.63	1.15
380	2.46	2.35	2.84	1.97
390	4.34	4.01	4.99	3.39
400	7.37	7.65	8.16	
410	12.16	12.61		
Activation energy (kJ mol^{-1})	200 ± 10	220 ± 10	190 ± 10	190 ± 10
Pre-exponential factor (s^{-1})	$(1.17 \pm 0.15) \times 10^{12}$	$(3.17 \pm 0.31) \times 10^{13}$	$(6.53 \pm 0.65) \times 10^{11}$	$(5.46 \pm 0.68) \times 10^{11}$

that traces of polymerisation catalyst in PET E and PET I affected the thermal stability. Antimony trioxide was used to polymerise PET I, but a different catalyst would have been used to give the higher DEG content present in PET E, and may be responsible, at least in part, for the reduced stability.

The activation energies and pre-exponential factors calculated from TA–FTIR data were higher than those calculated from TG data. The difference may be attributed to the fact that TG measures the overall weight change, as opposed to TA–FTIR spectroscopy, which monitors the loss of specific chemical groups. The inability to analyse changes in concentration of the aromatic units of the polyesters by TA–FTIR spectroscopy, more than anything else, probably caused the difference.

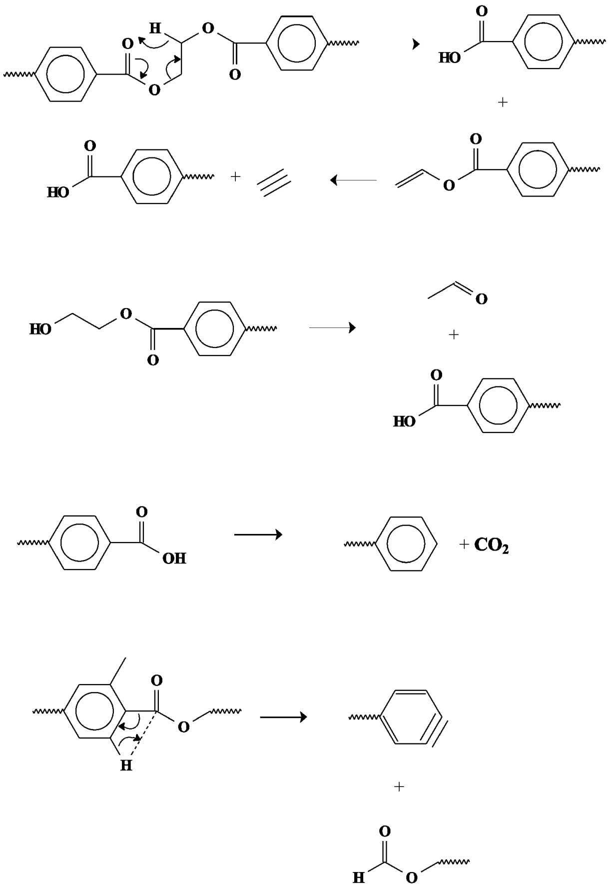

Fig. 21. Possible degradation mechanisms proposed for PET.

It was found that all the polyesters produced non-volatile residues. PET E and PET I produced yields of 18–20%, and appeared to be independent of the degradation temperature. TA–FTIR spectroscopic results indicate that the non-volatile residue was almost entirely made up of aromatic rings, and probably consisted of a network of interconnected aromatic rings, which originated from the phthalate segments of the original polymer. Aromatic groups constituted approximately 40 wt% of the original polymer, and typically 20 wt% residue was produced, it can be concluded that no more than 50% of the original aromatic structure was involved in producing the residue. Furthermore, all aliphatic groups in the PET were degraded to volatile fragments.

PEI and PDEGT produced non-volatile residues of 12–15%, but did not depend on the degradation temperature. The lower yield of residue in PEI and PDEGT was probably due to a back-biting degradation reaction being facilitated in the polymers, in PEI by the 1,3 substitution on the aromatic ring. This reduced ring strain in the cyclic product. Back-biting in PDEGT was facilitated by the additional flexibility of the DEG unit, compared to monoethylene glycol.

7. Conclusions

The thermal degradation of PET produces volatile degradation products and the formation of an non-volatile residue. The infrared spectrum of this showed that it consisted almost entirely of conjugated aromatic rings, probably six-membered, and substituted in combinations including 1,2,3- and 1,3-positions. The evolution of residue followed half order kinetics.

The mechanism of formation of the non-volatile residue was not fully resolved by TA–FTIR spectroscopic experiments. However, the results indicated that chain scission of both of the aliphatic linkages occurred, with subsequent

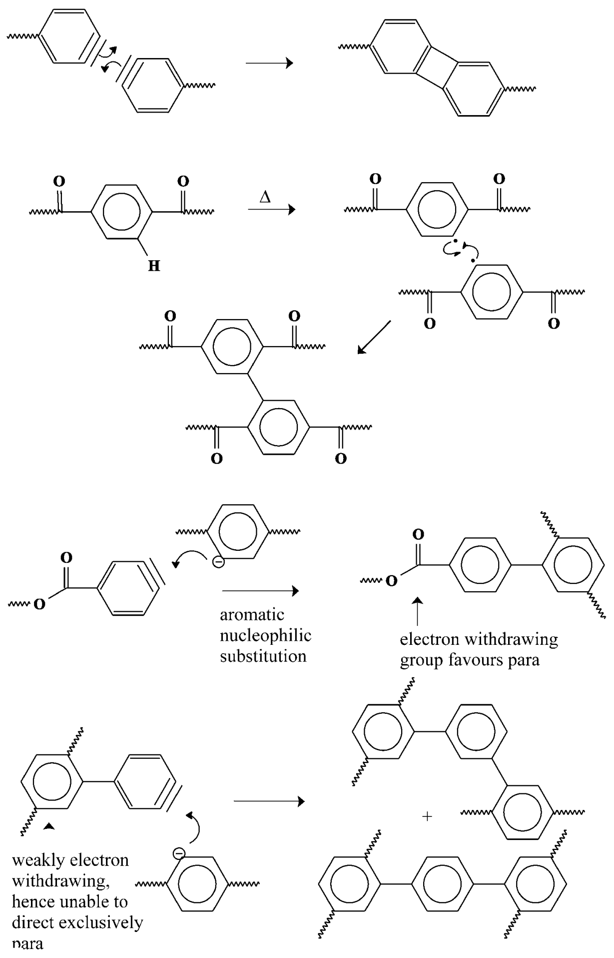

Fig. 22. Possible mechanisms of formation of aromatic network in PET.

volatilisation of the aliphatic parts. Furthermore, it is possible that hydrogen adjacent to the aliphatic linkages of the aromatic ring is acidic and probably thermally labile, and that elimination of substituents on the aromatic rings will lead to benzyne [20]. Benzyne reacts in one of two ways, the first involving aromatic nucleophilic substitution, and the second a Diels–Alder addition leading to *bis*-phenylene [21]. This information was used to produce the proposed mechanism of scission of the aliphatic side-chains (see Fig. 21), and the mechanisms of cross-linking proposed in Fig. 22.

It was found that the kinetics of elimination of the DEG end-groups did not follow those of other chemical groups in the polymer. DEG end-groups were more susceptible to thermal degradation than the polymer as a whole, and probably degraded via a five-membered transition state, producing acetaldehyde and an acid end-group.

PEI was also found to form volatile products and a non-volatile residue on thermal degradation. However, PEI produced less residue than PET, and it was considered that the volatile thermal degradation process in PEI was promoted by the more favourable angle of the 1,3-structure of the isophthalate unit for back-biting. The residue consisted almost entirely of aromatic rings.

Problems were encountered in the TA–FTIR study of PDEGT due to its low viscosity which allowed the polymer to flow during the spectroscopic experiments, and the resulting changes in absorbance made kinetic analysis meaningless. During thermal degradation, an infrared band developed at $3315\ \mathrm{cm}^{-1}$, which was associated with the formation of terminal carboxylic acid groups diethylene glycol end-groups.

References

[1] Sakellarides SL. Plast Engng 1996;52:33.
[2] Fann D-M, Huang SK, Lee J-Y. Polym Engng Sci 1998;38:265.
[3] Goodings EP. SCI Monogr 1961;13:211.
[4] Straus S, Wall LA. J Res Natl Bur Stds 1958;60:39.
[5] McNeill IC, Bounekhel M. Polym Degrad Stab 1991;34:187.
[6] Foti S, Giuffreda M, Maravigna P, Montaudo G. J Polym Sci Polym Chem 1984;22:1217.
[7] Montaudo G, Puglisi C, Samperi F. Polym Degrad Stab 1993;42:13.
[8] Luderwald I, Urrutia H. Makromol Chem 1976;177:2079.
[9] Adams RE. J Polym Sci 1982;20:119.
[10] Villain F, Coudane J, Vert M. Polym Degrad Stab 1994;43:431.
[11] Seo KS, Cloyd JD. J Appl Polym Sci 1991;42:845.
[12] Du Pont. Private communication. 1999.
[13] Holland BJ, Hay JN. Polymer 2001;42:4825.
[14] Rodig OR, Bell CE, Clark A. Organic chemistry laboratory—standard and microscale experiments. Orlando: Harcourt Brace Jovanovich Publishing, 1990. p. 280.
[15] Braun D, Cherdron H, Kern W. Techniques of polymer synthesis and characterisation. New York: Wiley-Interscience, 1972. p. 208.
[16] Bellamy LJ. The infrared spectra of complex molecules. 3rd ed. London: Chapman & Hall, 1975. p. 92.
[17] Bellamy LJ. The infrared spectra of complex molecules. 3rd ed. London: Chapman & Hall, 1975. p. 85.
[18] Boerio FJ, Bahl SK, McGraw GE. J Polym Sci Polym Phys 1976;14:1029.
[19] Bellamy LJ. The infrared spectra of complex molecules. 3rd ed. London: Chapman & Hall, 1975. p. 79.
[20] March J. Advanced organic chemistry. 4th ed. New York: Wiley-Interscience, 1992. p. 646.
[21] Sainsbury M. Aromatic chemistry, Oxford chemistry primers. Oxford: Oxford University Press, 1992. p. 30.